Experimental and Theoretical Study of Ventilation and Heat Loss From Isothermally Heated Clothed Vertical Cylinder in Uniform Flow Field

Nesreen Ghaddar[1]
Associate Provost
Qatar Chair in Energy Studies
Professor
American University of Beirut,
P.O. Box 11-0236,
Beirut 1107-2020, Lebanon
e-mail: farah@aub.edu.lb

Kamel Ghali
Associate Professor
American University of Beirut,
Beirut 1107-2020, Lebanon
e-mail: ka04@aub.edu.lb

Mohamad Al-Othmani
American University of Beirut,
P.O. Box 11-0236,
Beirut 1107-2020, Lebanon
e-mail: mha41@aub.edu.lb

Ingvar Holmer
e-mail: ingvar.holmer@design.lth.se

Kalev Kuklane
e-mail: kalev.kuklane@design.lth.se

Ergonomics and Aerosol Technology,
Lund University,
Box 118,
SE 211 00 Lund, Sweden

The flow characteristics and heat transfer are studied in a vertical annulus of a heated cylinder surrounded by a permeable cylinder, subject to cross uniform wind with open end to the environment and in the presence of natural convection. The objective here is to develop a computationally efficient model capable of capturing the physics of the flow and heat transport to predict air renewal rates in the vertical annulus. The small quantities of air infiltrating/exfiltrating through the porous cylinder over its upstream/downstream regions do not substantially affect the external flow pattern around the clothed cylinder. The air annulus flow and heat transport model predicted the radial and vertical mass fluxes and the mass flow rate at the opening as a function of environment conditions, porous cylinder thermal properties, wind speed, and annulus geometry. Experiments were performed in a low speed wind tunnel (0.5–5 m/s), in which an isothermally heated vertical cylinder surrounded by a clothed outer cylinder was placed in uniform cross wind. The tracer gas method is used to predict total ventilation flow rates through the fabric and the opening. Good agreement was found between the model and experimental measurements of air renewal rate and predicted heat loss from the inner cylinder at steady conditions. A parametric study is performed to study the effect of wind speed and temperature difference between the wind and skin temperature on induced ventilation through the clothing and the opening. It is found that natural convection enhances ventilation of the annulus air at wind speed, less than 3 m/s, while at higher speeds, natural convection effect is negligible. As the temperature difference between external wind and inner cylinder surface increases, the vertical air temperature gradient and total upward airflow through the opening increase. [DOI: 10.1115/1.4000429]

Keywords: mixed convection in vertical annulus, clothed vertical heated cylinder ventilation, airflow through porous cylinder

1 Introduction

The flow characteristics and heat transfer of induced airflow in the vertical annulus of a heated cylinder surrounded by an impermeable cylinder with open-end or closed aperture are well established in literature [1–5]. The flow characteristics in the vertical annulus become complicated when the outer cylinder is a porous thin boundary subject to uniform crosswind, resulting in mixed convective upward flow in the annulus. The penetrating/ventilating airflow from the environment through the thin porous cylinder will change flow characteristics in the air layer and the associated heat loss from the inner heated cylinder when compared with the case of vertical annular natural convection driven flow at zero wind. This solution of this problem can be widely used as a standard model configuration of a clothed human trunk or limb to study local body segment ventilation, which is essential for estimation of heat and moisture transport from the skin, thermal comfort, and protection offered by the clothing [6–9]. Sobera et al. [6] focused their 2D study on heat and mass transfer from horizontal clothed cylinder, sheathed by a porous layer placed in turbulent flow to represent clothed human limb. Kind et al. [7] reported experimental heat transfer results from fabric covered cylinders, and Gibson [8] and Leong and Lai [9] reported numerical computations of free and mixed convection around the fabric covered cylinders. These studies reported on the laminar flow characteristics in the annular trapped air layer and the convective heat loss, but did not consider mixed and natural convection in a 3D vertical air annulus flow for a fabric covered cylinder in cross flow and with open-end aperture. This configuration has received much less attention. Some relevant work on this fundamental problem was reported by Chaves et al. [10], who numerically analyzed heat transfer inside a 2D semiporous cavity between two vertical walls, open at the top and closed at the bottom, by a uniform heat flux horizontal wall. The cavity had one vertical porous wall with a normal forced fluid flowing through it, and the other vertical wall is impermeable at uniform heat flux [10]. They showed how the natural convection has improved the forced convection inside the open cavity induced by flow from the boundary.

At present, no study has been performed that includes the effect of natural convection and is derived from first principles of air annulus microclimate ventilation and heat transport from a clothed vertical cylinder as a function of all the relevant physical and geometric parameters. In this work, we present a dry model of coupled ventilation and heat mixed convection in a vertical air annulus between concentric fabric cylinder and heated solid cylinder placed in perpendicular to airflow. The model will be vali-

[1]Corresponding author.

Contributed by the Applied Mechanics Division of ASME for publication in the JOURNAL OF APPLIED MECHANICS. Manuscript received March 23, 2009; final manuscript received July 31, 2009; published online February 23, 2010. Editor: Robert M. McMeeking.

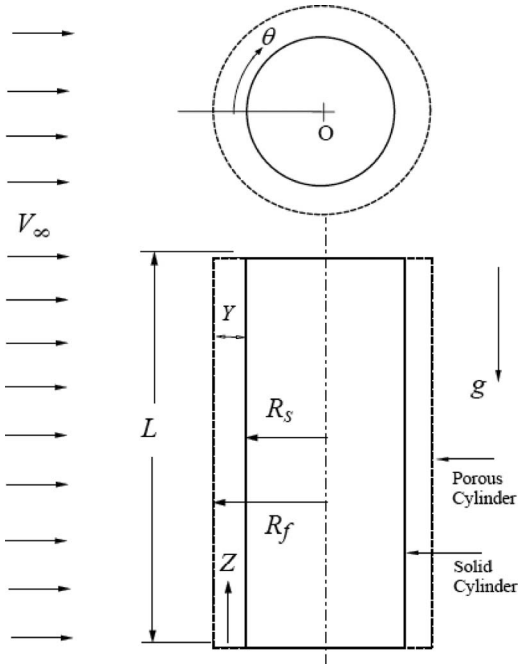

Fig. 1 The physical configuration of the clothed vertical cylinders of radii R_s and R_f and height L

dated by experiments and will be followed by a parametric study to address how external wind and natural convection alter heat and mass transfer from the inner clothed and heated cylinder. The generality of the formulation will make it valid for many different applications including the ventilation of a walking clothed human trunk.

2 Mathematical Formulation

2.1 Physical Model and Governing Equations. The physical configuration of the present study shown in Fig. 1 consists of two concentric vertical cylinders of radii R_s and R_f and height L. A microclimate air annulus of thickness $Y=(R_f-R_s)$ is trapped between the inner solid cylinder maintained at temperature T_{skin} and the outer porous cylinder represented by an isotropic fabric layer of permeability α and thickness e_f. The bottom end of the annulus is closed and adiabatic, while the top end is open to the environment at temperature T_∞. The configuration is placed in perpendicular to an air flow at V_∞. Some air penetrates through the porous fabric into the air layer and is driven upward by an existing pressure gradient, due to the presence of the opening and natural convection. The steady flow into the microclimate through the fabric is very small compared with the external wind flow and is laminar [6,11]. The external pressure distribution around the clothed cylinder is not influenced by the presence of the clothing cover as can be deduced from studies on flow around cylinders sheathed by clothing. Sobera et al. [6] and Kind et al. [7] reported experimental measurements of static pressures on a clothed cylinder surface, showing that the small quantities of air infiltrating/exfiltrating through the sheath over its upstream/downstream regions did not significantly affect the external flow pattern. Watanabi et al. [12] reported that the velocity distribution around the clothed cylinder was hardly influenced by clothing, except for the shift of the separation point for fabric permeability of order 10^{-10} m^2. The annulus trapped air thickness Y is small compared with the length and radius of the inner cylinder ($Y \ll L$ and $Y \ll R_s$), which permits the assumption of fully developed mixed buoyant upward flow [5,13] and the angular flow with negligible pressure variations in the radial direction [11]. With these assumptions and under conditions of incompressible Boussinsq fluid of constant thermophysical properties, the formulation of the 3D problem of the coupled momentum and heat transfer in the vertical annulus will be transformed into a 2D problem of coupled energy balance and pressure equation, derived from mass and momentum equations [14]. The thermal analysis will be focused on dry analysis, where water vapor adsorption in the fabric and changes in trapped air layer humidity ratio are not considered.

The mathematical formulation starts with the air annulus mass conservation equation given by

$$\frac{\partial(Y\dot{m}_{az})}{\partial z} + \frac{\partial(Y\dot{m}_{a\theta})}{R_f \partial \theta} + \dot{m}_{aY} = 0 \tag{1}$$

where $\dot{m}_{az}$ is the mass flux in the vertical z-direction in kg/m^2 s, $\dot{m}_{a\theta}$ is the mass flux in the angular θ-direction, and $\dot{m}_{aY}$ is the radial infiltrating air flow rate through the fabric given by

$$\dot{m}_{aY} = \frac{\alpha \rho_a}{\Delta P_m}(P_a - P_s) \tag{2}$$

where α is the fabric air permeability expressed in m^3/m^2 s, as normally used in testing fabrics [1], $\Delta P_m = 0.1245$ kPa from standard tests on fabrics' air permeability [1], P_a is the air pressure in the microclimate trapped air layer (kPa), and P_s is the external adjacent air layer pressure (kPa). The external fabric pressure that drives the radial flow is assumed to be the same pressure distribution that results from a flow around a circular cylinder at flow condition V_∞. Assuming a Poiseuille flow model in the angular horizontal direction; the mass angular air mass flow rate per unit area is expressed in terms of the annular pressure as

$$\dot{m}_{a\theta} = -\frac{Y^2}{12 R_f \nu}\frac{dP_a}{d\theta} \tag{3}$$

where ν is the air kinematic velocity. In the upward flow, we use the second order momentum equation for developing flow in the vertical cavity with driving pressure term, due to forced flow and the induced buoyant pressure term [5], to obtain the vertical mass flow rate per unit area in terms of pressure and driving temperature gradient of the air and temperature difference between the inner wall and the infiltrating air. The second order momentum equation is given by

$$\nu\frac{d^2u}{dy^2} = \frac{dP_a^*}{dz} - g\beta(T_a - T_R) \tag{4}$$

where u is the physical velocity across Y, P_a^* is the modified $P_a^* = P_a + \rho_a g z$, β is the volumetric thermal expansion coefficient, g is the gravitational acceleration, T_a is the air layer temperature, and T_R is the reference temperature taken at the temperature of the penetrating air flow from the fabric void T_{void} [10]. Solving the above equation subject to no slip condition for u results in a parabolic velocity distribution that can be integrated across the gap width to obtain the vertical mass flux rate per unit area as

$$\dot{m}_{az} = -\frac{Y^2}{12\nu}\frac{dP_a^*}{dz} + \frac{g\beta Y^2}{12\nu}(T_a - T_{\text{void}}) \tag{5}$$

The radial, angular, and upward mass flow rates of Eqs. (2), (3), and (5) are substituted in Eq. (1) to get the mass conservation equation as a pressure equation coupled to driving temperature difference between the air layer and its boundaries given by

$$\frac{\alpha(P_s - P_a)}{\Delta P_m} + \frac{\partial}{R_f^2 \partial \theta}\left(\frac{Y^3}{12\nu}\frac{\partial P_a}{\partial \theta}\right) + \frac{\partial}{\partial z}\left(\frac{Y^3}{12\nu}\frac{\partial P_a^*}{\partial z}\right) - \frac{\rho_a g \beta Y^2}{12\nu}[T_a - T_{\text{void}}] = 0 \tag{6}$$

The steady state dry energy balance on the air spacing annulus is a balance of (1) the dry convective heat transfer from the surface of the inner cylinder, (2) the heat flow to the air layer associated with mass fluxes from the radial, angular, and vertical di-

rections $\dot{m}_{aY}$, $\dot{m}_{a\theta}$, and $\dot{m}_{ax}$, (3) the heat diffusion from void air of the thin fabric to the air layer, and (4) the angular conduction of heat in the air layer. The dry energy balance of the air layer is then given by

$$h_{c(\text{skin-air})}(T_{\text{skin}} - T_a) + h_{c-o}(T_o - T_a) - \dot{m}_{aY}H_p - \frac{\partial(Y\dot{m}_{az}C_pT_a)}{\partial z} + \frac{\partial[Y\dot{m}_{a\theta}C_pT_a]}{R_f\,\partial\,\theta} + \frac{k_a}{R_f^2}\frac{\partial}{\partial\theta}\left(Y\frac{\partial T_a}{\partial\theta}\right) + k_aY\frac{\partial^2 T_a}{\partial z^2} = 0 \tag{7a}$$

$$H_p = \begin{cases} C_pT_{\text{void}} & P_a < P_s \\ C_pT_a & P_a > P_s \end{cases} \tag{7b}$$

where $h_{c(\text{skin-air})}$ is the convection coefficient from the skin to the air [1], $h_{c(o-\text{air})}$ is the convection coefficient from the fabric to the air, T_o is the fabric outer node temperature [1], k_a is the thermal conductivity of air in the trapped air annulus, and C_p is the air specific heat. The internal heat transfer convective coefficients for mixed convection, which ranged between 9.6 $\text{W/m}^2\,\text{K}$ and 10.5 $\text{W/m}^2\,\text{K}$, are obtained from empirical data reported on local Nusselt number variation in the axial direction by Mohanity and Dubey [1] and verified by correlations reported by Reddy and Narasimham [15].

The outer fabric cylinder will be modeled using the three-node-fabric model of Ghali et al. [16,17], which uses a lumped layer of two fabric nodes (inner and outer) and an air void node to represent the thin fabric medium. The fabric outer node represents the exposed surface of the yarns, which is in direct contact with the penetrating air in the void space (air void node) between the yarns. The fabric inner node represents the inner portion of the "solid" yarn surrounded by the fabric outer node. Since we have steady state conditions, the fabric inner and outer nodes will be at thermal equilibrium, and the energy balance on the fabric will modify Ghali et al. [16] to include only the dry balance on the fabric void node and the fabric outer node as follows:

$$\text{Fabric void node} \quad H'_{\text{co}}(T_o - T_{\text{void}}) + \dot{m}_{aY}H_e = 0 \tag{8a}$$

$$H_e = \begin{cases} C_p(T_\infty - T_{\text{void}}) & P_a < P_s \\ C_p(T_a - T_{\text{void}}) & P_a \geq P_s \end{cases} \tag{8b}$$

$$\text{Fabric outer node:} \quad h_{c(o-a)}(T_\infty - T_o) + H'_{\text{co}}(T_{\text{void}} - T_o) + \frac{h_r}{2}(T_{\text{skin}} - T_o) + \frac{h_r}{2}(T_\infty - T_o) = 0 \tag{8c}$$

where H'_{co} is the effective void space heat transfer coefficient between air passing through the void and the fabric outer node (yarns) [17], h_c is the external heat transfer coefficient between the fabric outer node and the environment, and h_r is the linearized radiative heat transfer coefficient, and its value ranged between 3.5 $\text{W/m}^2\,\text{K}$ and 4 $\text{W/m}^2\,\text{K}$ [18].

2.2 Boundary Conditions. The associated boundary conditions for the air flow are given by

$$\dot{m}_{az}(z=0,\theta) = 0 \;\&\; \dot{m}_{az}(z=L,\theta) = C_D[2\rho_a(P_L - P_\infty)]^{1/2} \tag{9a}$$

$$\dot{m}_{a\theta}(z, \theta = 0 \quad \text{or} \quad \pi) = 0 \tag{9b}$$

where Eq. (9*a*) is derived from the pressure drop at the opening by applying Bernoulli's equation from P_∞ in the far environment ($z \to \infty$) to the opening at $z=L$, and C_D is the discharge loss coefficient at the aperture of the domain dependent on the discharge area ratio of the aperture to the air layer thickness Y, which is in unity in this problem.

Considering the inner cylinder is isothermal at T_{skin} and the environment temperature is at T_∞, the associated thermal boundary conditions for the air layer annulus second order energy equation are given by

$$\frac{dT_a}{dz}(z=0,\theta) = 0 \quad \text{and} \quad \frac{dT_a}{dz}(z=L,\theta) = 0 \tag{10a}$$

$$\frac{dT_a}{d\theta}(z, \theta = 0 \quad \text{and} \quad \theta = \pi) = 0 \tag{10b}$$

The opening boundary condition for the temperature in the z direction assumed to be a fully developed thermal profile exiting the domain and is similar to conditions used by other researchers [10].

2.3 Numerical Solution. The coupled pressure and energy Eqs. (6)–(8) are discretized using a finite volume methodology, where the air layer computational zone is divided into $N_z \times N_\theta$ grids of size Δz and $R_f\Delta\theta$ with thickness Y, as shown in Fig. 2. The discrete air pressure and temperature at the volume center notations are

$$P_{a(i,j)} = P_a\left(\frac{z_{i-1,j} + z_{i,j}}{2}, \frac{\theta_{i,j-1} + \theta_{i,j}}{2}\right) \qquad \{i = 0,\ N_z \quad \text{and} \quad j = 0,\ N_\theta\}$$
$$T_{a(i,j)} = T_a\left(\frac{z_{i-1,j} + z_{i,j}}{2}, \frac{\theta_{i,j-1} + \theta_{i,j}}{2}\right) \tag{11}$$

and the discrete facial air mass flow rates notations are

$$\dot{m}_{az(i,j)} = -\frac{Y^2}{12\nu}\frac{(P^*_{a(i,j)} - P^*_{a(i-1,j)})}{\Delta z} + \frac{g\beta Y^2}{12\nu}(T_{a(i,j)} - T_{\text{void}(i,j)}) \tag{12a}$$

$$\dot{m}_{a\theta(i,j)} = -\frac{Y^2}{12R_f\nu}\frac{(P_{a(i,j)} - P_{a(i,j-1)})}{\Delta\theta} \tag{12b}$$

The discrete model equations for the air layer pressure and energy equations balance for any internal node in the computational domain are given by

$$\frac{\alpha(P_{s(i,j)} - P_{a(i,j)})}{\Delta P_m} + \frac{Y^3}{12\nu R_f^2}\left(\frac{P_{a(i,j-1)} - 2P_{a(i,j)} + P_{a(i,j+1)}}{\Delta\theta^2}\right) + \frac{Y^3}{12\nu}\left(\frac{P^*_{a(i-1,j)} - 2P^*_{a(i,j)} + P^*_{a(i+1,j)}}{\Delta z^2}\right) - \frac{\rho_a g\beta Y^2}{12\nu}[T_{a(i,j)} - T_{\text{void}(i,j)}] = 0 \tag{13a}$$

$$h_{c(\text{skin-air})}(T_{\text{skin}} - T_{a(i,j)}) + h_{c-o}(T_{o(i,j)} - T_{a(i,j)}) - \dot{m}_{aY(i,j)}H_{p(i,j)} - YC_p\frac{(\dot{m}_{az(i+1,j)}T_{a(i+1,j)} - \dot{m}_{az(i,j)}T_{a(i,j)})}{\Delta z} + \frac{YC_p}{R_f}\frac{(\dot{m}_{a\theta(i,j+1)}T_{a(i,j+1)} - \dot{m}_{a\theta(i,j)}T_{a(i,j)})_a}{\Delta\theta} + k_aY\frac{T_{a(i-1,j)} - 2T_{a(i,j)} + T_{a(i+1,j)}}{\Delta z^2} + \frac{k_aY}{R_f^2}\left(\frac{T_{a(i,j-1)} - 2T_{a(i,j)} + T_{a(i,j+1)}}{\Delta\theta^2}\right) = 0 \tag{13b}$$

where central differencing is used for second order terms in the air layer pressure and energy equations. An initial guess for the air temperature values for all nodes is assumed. The pressure equation is solved for pressure nodal values at this air temperature while assuming the value of the exit pressure $P_a(Nz, j)$ to implement the Bernoulli equation (9*a*) assumed at the open annulus boundary. Mass flow rates are calculated and then substituted in the energy equations to update the nodal values of the temperature domain. This iterative process is repeated until convergence is

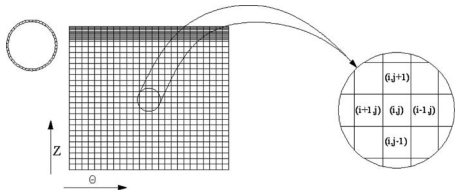

Fig. 2 The computational domain and grid distribution

reached when both coupled pressure and temperature equations converge, such that overall mass and energy are conserved in each grid and values of pressure and temperature to a minimum relative error of 10^{-5} of all dependent parameters including opening values. Given the pressure distribution in the air layer and temperature distributions of the air layer, and the fabric void and the fabric outer node, the mass flow rates of all directions are calculated to estimate ventilation rates and to predict the dry heat loss from the inner cylinder surface. The numerical solution is repeated for grid sizes to ensure that a grid-independent solution is obtained. In the presented simulations, the number of grid points was 400, with a maximum $\Delta\theta$ of 1 deg and minimum Δz of 0.001 m close to the opening. The total heat loss from the inner surface is then evaluated as

$$Q = \sum_{i=1}^{N_\theta} \sum_{j=1}^{N_z} h_{\text{skin-air}(i,j)} R_s \Delta_\theta \Delta_z (T_{sk} - T_{a(i,j)}) + h_{r(i,j)} R_s \Delta_\theta \Delta_z (T_{sk} - T_{o(i,j)}) \quad (14)$$

where h_r is the linearized radiative heat transfer coefficient.

2.4 Definition of Microclimate Ventilation Rates. Of interest is to calculate the total ventilation rate of the fabric, based on the renewal rate induced by external wind penetrating the porous fabric and enhanced by buoyancy. The total ventilation rate is calculated as the positive flow of air into the air annulus integrated per unit area of the clothed surface as follows:

$$\dot{m}_a = \frac{1}{2\pi L} \int_0^L \int_0^{2\pi} \max(0, \dot{m}_{aY}) d\theta dz \ \text{kg/s m}^2 \quad (15a)$$

In the above integral, $\dot{m}_{aY}$ is equated to zero when it is negative (flowing out of the microclimate). The air flow out of the top open aperture is also calculated per unit area of clothed surface during the period of motion as

$$\dot{m}_o = \frac{Y}{2\pi L} \int_0^{2\pi} \dot{m}_{az(z=L)} d\theta \ \text{kg/s m}^2 \quad (15b)$$

where $\dot{m}_o$ is the upward flow rate through the open aperture.

3 Experimental Methodology

This section presents the experimental setup used for measuring the steady annulus microclimate ventilation rates and heat losses from a heated clothed cylinder in stagnant air and in uniform cross wind. Untreated cotton with permeability of 0.05 m^3/m^2 s was chosen as a representative of the most common worn fabric. The cotton was obtained from Test Fabrics Inc. (Middlesex, NJ 08846) and is made of unmercerized cotton duck, style No. 466 with thickness of 1 mm.

The uniform cross wind experiments over the clothed swinging cylinder were conducted using a low speed wind tunnel. The wind tunnel uses a blow type variable speed three-phase axial fan with 0.7 m in diameter and peak power of 1.6 kW. The square test cross section dimensions were 0.8×0.8 m^2. In order to obtain the uniform velocity profile inside the tunnel, a porous metal screen was used as a flow straightener after the tunnel diffuser section. The uniform wind provided in the wind tunnel ranged from 0.5 m/s to 6 m/s, giving a Reynolds number range from 4000 to 40,000, based on the limb diameter. The spatial variation in the free stream velocity in the wind tunnel cross section was measured using a hotwire anemometry system and was found to vary within 4% of its spatially averaged value within the cross section, and the turbulence intensity was 2–3%.

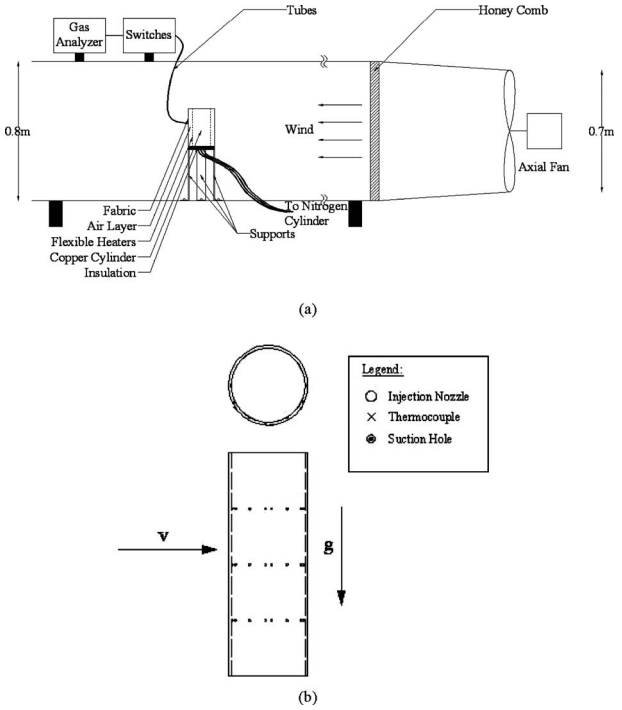

Fig. 3 Schematic of (*a*) the clothed heated vertical cylinder setup in the low speed wind tunnel and (*b*) the location of the N_2 injection, N_2 suction holes, and the mounted thermocouples

Figure 3(*a*) shows a schematic of the clothed heated vertical cylinder experimental setup, measurement systems, and components. The clothed cylinder setup consisted of: (i) a copper hollow inner cylinder with a diameter of 0.104 m and a length of 0.215 m; (ii) an outer fabric 0.215 m long and 0.139 m diameter cylinder made of a thin metallic screen of 2 cm open squares, where the cotton fabric is wrapped around and tightly fitted; (iii) support platform; and (iv) Styrofoam insulative material to insulate the bottom of the vertical cylinder. The concentric cylinders are fixed at the lower end to the supporting insulated frame.

The inner cylinder is wrapped with metallic resistance heaters Omega-KH-1012 to produce constant heat flux condition per heater at the cylinder surface. The heat fluxes from the heaters are regulated independently, such that an almost uniform mean steady temperature of $33\,^\circ\text{C} \pm 0.5\,^\circ\text{C}$ is attained for each strip heater due the high conductivity of the surface heaters. Thermistors of type Omega-44133 are placed in small microgrooves in the inner cylinder surface and at five angular locations of front (θ=0 deg), sides (θ=45 deg, 90 deg, and 135 deg), and back (θ=180 deg) for three heights of z=0.055 m, 0.108 m, and 0.166 m, and close to the opening at z=0.205. The heat flux elements on the surface are thermally conducting. This has resulted in a closely uniform inner surface temperature, and the maximum measured skin temperature difference between the three positions was less than $0.3\,^\circ\text{C}$. Other radiation-shielded thermistors of type Omega-44133 are placed within the air gap and about 0.5 cm from the outer circumference toward the center at θ=0 deg, 45 deg, 90 deg, and 135 deg, and θ=180 deg for z=0.055 m, 0.108 m, and 0.166 m. The accuracy of the temperature readings was $\pm 0.1\,^\circ\text{C}$.

The microclimate ventilation rate is measured using the tracer gas method for closed and open aperture. The tracer gas method is

used, as described by Havenith et al. [19]. The gas chosen must have a density that is close to that of air. This is to ensure that we will have no stratification. The measurements are done by radially injecting an inert gas (N_2) at a fixed rate through the nozzles placed at holes drilled in the inner cylinder surface between the resistance heaters, as shown in Fig. 3(*b*). The concentration of the oxygen gas is measured in the air gap at different angular and axial locations using a standard exhaust gas analyzer (Emissions Systems Inc., Illinois, EMS Model 4001). Ten small diameter (5 mm) flexible tubing with end probes, to draw air samples, are positioned in three axial locations (three probes for each axial position distributed uniformly around the circumference) at $z=0.055$ m, 0.108 m, and 0.166 m. The probes draw samples of air from a radial distance of 4 mm in the air layer away from the fabric outer cylinder. A switch board is designed to draw air sample for O_2 concentration measurements for different locations by switching from one tubing-probe system to the other without interfering with the air flow around the arm. The gas analyzer measurements have an accuracy of $\pm 0.05\%$ of volume of O_2 of the air sample. The nitrogen gas is injected by a flow regulator that injects nitrogen into the air layer at $1.0L/s$ and $1.5L/s$ from a pressurized nitrogen vessel with precision of $\pm 0.01L/s$. The standard air sample composition by volume is 79% N_2 and 21% O_2. To obtain the concentration of N_2 in the microclimate, the recorded concentration of O_2 is deducted from the 100%. The total volume flow rate renewal can be calculated from the trace gas mass flux ψ_{tr} (m^3/s), the measured concentrations C_a (m^3 O_2/m^3 air), and C_∞ (m^3 O_2/m^3 air) at the inner and outer locations, respectively, as

$$\frac{\overline{\dot{m}_a}}{\rho_a}[C_\infty - C_a] + \psi_{tr} = 0 \tag{16}$$

The lab, where the wind tunnel experiments are performed, is well ventilated, and the environmental chamber air was refreshed frequently between experiments to prevent nitrogen concentration buildup in the chamber. The actual uncertainty in the determination of the experimental ventilation mass flow rate $\overline{\dot{m}_a}$ can be found from the uncertainties in the injection rate ψ_{tr} and measured concentrations C_a and C_∞ as

$$\Delta\overline{\dot{m}_a} = \pm \sqrt{\left[\left[\frac{\partial\overline{\dot{m}_a}}{\partial\psi_{tr}}\cdot\Delta\psi_{tr}\right]^2 + \left[\frac{\partial\overline{\dot{m}_a}}{\partial C_\infty}\cdot\Delta C_\infty\right]^2 + \left[\frac{\partial\overline{\dot{m}_a}}{\partial C_a}\cdot\Delta C_a\right]^2\right]} \tag{17}$$

Experiments were conducted for 0.5 m/s, 1 m/s, 2 m/s, and 4 m/s crosswind when heaters are on and when they are not to determine the effect of natural convection that occurs in the annulus between the heated inner cylinder and the outer porous fabric. In each experiment, the flow is maintained for at least 1 h to reach thermal steady state before a steady injection of $1.0L/s$ of N_2 through the holes of the inner cylinder was started. Steady conditions of gas concentrations were reached after 1 h from the onset of N_2 injection. Data was recorded every 10 min. The experiments were repeated at different N_2 injection rates of $1.5L/s$ to check the homogeneity of the calculated N_2 concentration inside the annulus and repeatability of the O_2 concentration measurements. The actual uncertainty in $\Delta\overline{\dot{m}_a}$ in the range of the reported experimental values of the ventilation mass flow rate (0.5–5 g/s) was found to be less than ± 0.02 g/s. Measurements of temperature of the air annulus for the various experiments are recorded. In each case, the input heat flux and temperatures of the inner cylinder surface were also monitored.

4 Results and Discussion

This section presents the computational and experimental results of ventilation rates and heat loss from a clothed vertical cylinder and is divided into two subsections. The first subsection is concerned with microclimate ventilation and heat loss model validation with experiments. The second is concerned with a parametric study of the effects of wind and geometric and physical parameters on ventilation rates and heat loss from the inner cylinder.

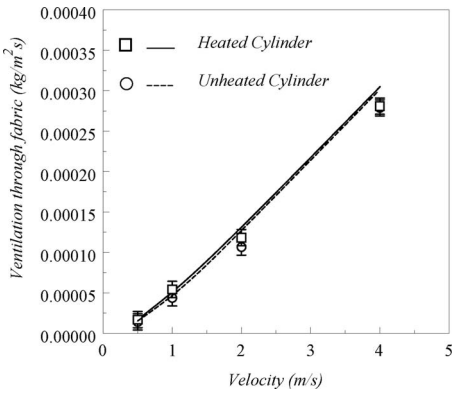

Fig. 4 A plot of the model predictions and experimentally obtained opening and normal ventilation rates cross wind speed of 0.5 m/s, 1, 2 m/s, and 4 m/s with and without heating at for environmental conditions of $T_\infty = 22°C$ and inner cylinder surface temperature of $T_s = 33.5°C$

4.1 Model Validation by Experiments. The clothed vertical cylinder geometry was simulated at the environmental and physical conditions of the experiments using current proposed coupled mass and energy balances of the annulus air and energy balances on the fabric nodes. The model predicted opening and total ventilation rates, the air annulus temperature distribution, and the associated heat loss from the inner cylinder to compare with experimentally measured values.

Figure 4 shows a plot of the model predictions and experimentally obtained overall normal ventilation rates per unit of fabric area in cross wind speed of 0.5 m/s, 1 m/s, and 2 m/s, with and without heating for environmental conditions of $T_\infty = 22 \pm 0.5°C$ and inner cylinder surface temperature of $T_s = 33.5 \pm 0.5°C$. Observations are made here on the agreement between experimental data and model predictions and on the enhancement of ventilation when aided by natural convection, particularly at low wind speeds. Good agreement, within 5% error, is found between the predicted ventilation and measured ventilation. The agreement between experiments and model predictions improves at higher wind speed as less effect of accumulation of tracer gas concentration in the outer environment due to the blowing wind. To check the sensitivity of the model to error in used skin temperature, simulations are performed at inner cylinder temperatures of 32.5°C and 33.5°C, and the heat loss was differed by less than 4% from the value obtained at 33°C. The heat loss for the case of zero wind and zero motion was 30.02 W/m^2. This value is close to the reported measured mean heat loss of 24 W/E^2 from a standing subject with transmitting garment that has different dry and evaporative resistances than the fabric used in our experiments [20]. In the presence of natural convection, the ventilation is substantially enhanced at low external wind velocities, where at wind speed of 0.5 m/s, the ventilation rate for a heated vertical cylinder is enhanced by 13% compared when no natural convection is present (unheated cylinder). At wind speed of 2 m/s, the enhancement in ventilation rate is less than 5%.

Figure 5 shows the predicted and experimentally measured values of (a) angular-averaged air annulus temperature as a function of height at wind speed of 2 m/s, and (b) the total power input to the heated surface as a function of wind velocity at surface temperature of 33.5 °C and environment temperature of 22°C. The agreement between the experimental measurements of the air temperature and model predictions of the air layer temperature has shown a relative error between 4% and 6%. This is expected since

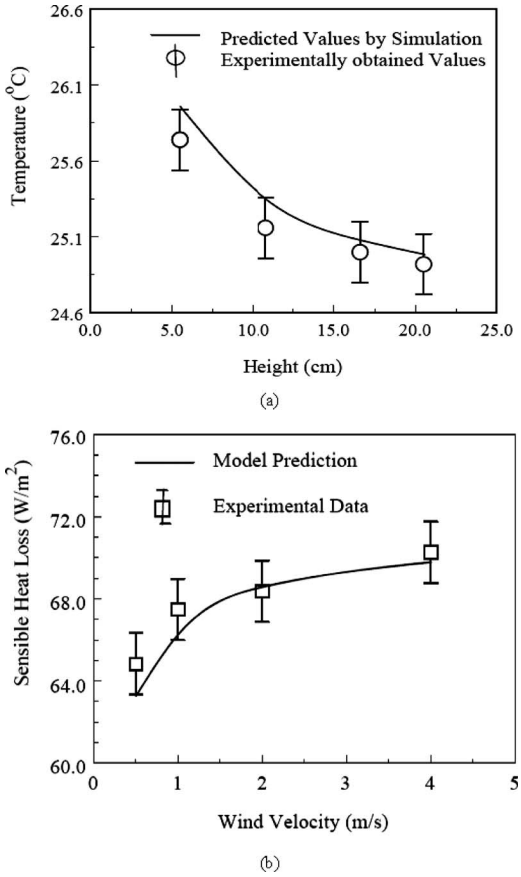

Fig. 5 Plots of the predicted and experimentally measured values of (*a*) angular-averaged air annulus temperature as a function of height at wind speed of 2 m/s and (*b*) the total power input to the heated surface as a function of wind velocity at surface temperature of 33.5°C and environment temperature of 22°C

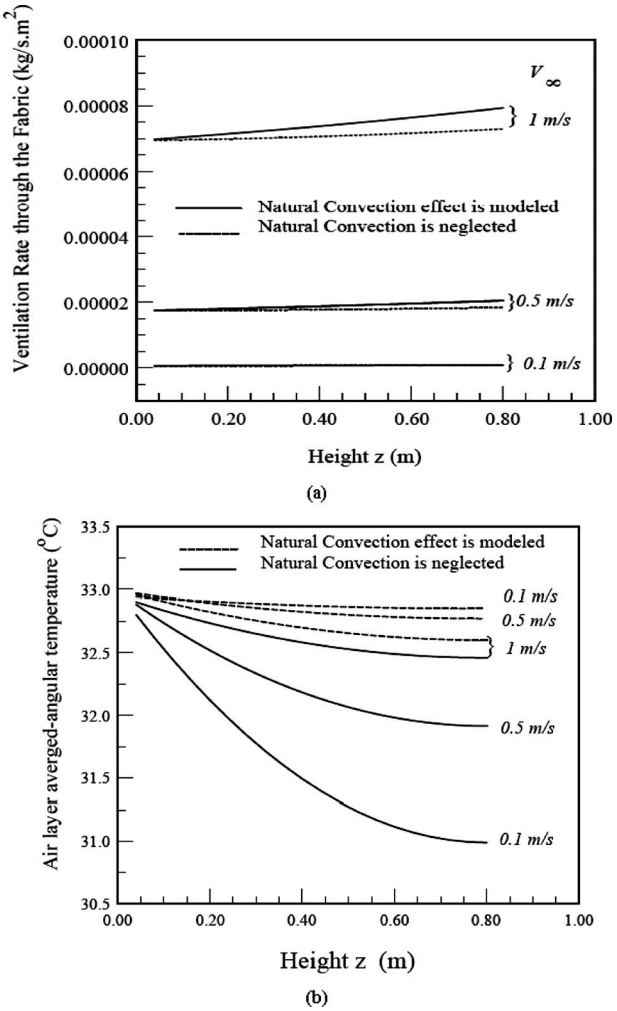

Fig. 6 Plots of (*a*) the normal ventilation rate through outer fabric and (*b*) the air annulus angular-averaged temperature as a function of cylinder height for both models with and without natural convection effect at fabric permeability of 0.05 m/s and ambient temperature of 25°C

the model of the air layer is a lumped model, while measurements of air layer are taken at a local point in the air annulus where the thermocouple is placed at 0.5 cm away from the outer surface. The average air annulus temperature decreases with increased ventilation, which explains the increase of heat loss from the inner cylinder with increased external wind.

4.2 Parametric Study and Factors That Affect Heat Transfer Increase for Mixed Convection. It is of interest to recognize the principal mechanism of ventilation in the microclimate annulus between a solid and porous cylinder at various wind conditions and investigate the effect of porous cylinder air permeability and driving temperature difference for natural convection flow. We would like to explore the wind conditions above which the natural convection effect on enhancing ventilation and heat loss is insignificant. A clothed cylinder with inner cylinder diameter of 0.2636 m, height of 0.8 m, and gap width of 0.01 m is selected to perform simulations at inner cylinder surface temperature of 33.0°C, using our developed model to predict local distributions and space-averaged values of ventilation rate through the fabric and at the top opening, air and fabric temperature, and sensible heat loss as a function of wind speed, ambient temperature, and fabric permeability in the presence of natural convection, and when the effect of natural convection is neglected. The threshold of external wind above which natural convection can be neglected is also found as function of temperature difference between the heated cylinder surface and environment.

Figure 6 shows, as a function of cylinder height, (a) the normal ventilation rate through the outer fabric and (b) the air annulus angular-averaged temperature for both models with and without natural convection effect at fabric permeability of 0.05 m/s and ambient temperature of 25°C. Figure 7 shows, as a function of the cylinder height, the air annulus angular-averaged temperature at different ambient conditions for both models, with and without natural convection effect at fabric permeability of 0.05 m/s and wind speed of 0.5 m/s. The presence of natural convection enhances ventilation in the fabric by inducing higher upward velocity, hence creating lower air layer pressure. The lower pressure in the air annulus drives more radial flow though the fabric (see Fig. 6(*a*)), and hence reduces air layer temperature with height, as shown in Fig. 6(*b*). The higher the wind speed, the higher is the ventilation rate through the fabric. However, the air layer temperature decreases with height to reach the lowest value at the opening. The air layer negative temperature gradient is largest at 1 m/s, and as wind velocity increases, the temperature gradient is smaller. The angular-averaged air temperature at the opening is shown in Fig. 8 as a function of wind velocity at ambient condition of 25°C, with and without natural convection effect. At higher speed, the predictions of opening temperature and ventilation rates by the model with and without natural convection approach each other. The opening temperature decreases with increased wind speed. When natural convection is taken into consideration, the opening temperature is lower than the case

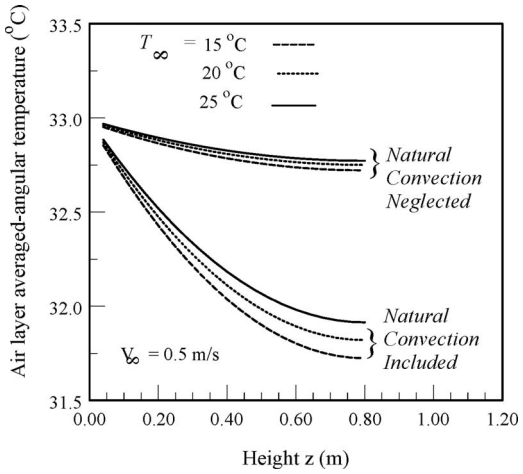

Fig. 7 Plot of the air annulus angular-averaged temperature as a function of cylinder height at different ambient conditions for both models with and without natural convection effect at fabric permeability of 0.05 m/s and wind speed of 0.5 m/s

when buoyancy is neglected, but converges to the same value of temperature when wind speed is 5 m/s. The increase in vertical annulus flow driven by natural convection draws in higher radial ventilation rates that cool the upward flow faster as it reaches the opening at the top.

The effect of incorporating of natural convection on total ventilation rate per unit area of the cylinder surface and on the heat loss from the cylinder of the inner cylinder is carefully considered for a variety of conditions of the environment and at different fabric permeabilities. Figure 9 shows (a) the total ventilation rate through the fabric as predicted by the mixed convection model as a function of wind velocity at various fabric permeabilities and (b) the corresponding % increase in ventilation when natural convection is incorporated. For wind velocities above 2.5–3 m/s, natural convection can be neglected in the model with error in ventilation that is less than 5–3%, respectively.

Figure 10 shows the total heat loss through the fabric as predicted by the mixed convection model as a function of wind velocity at various fabric permeabilities. The corresponding % increase in heat loss when natural convection is included ranged from 12% to 7%, depending on the permeability. For higher permeability fabric, the natural convection enhancement effect on heat loss prediction is more important than that encountered at low permeability fabric. This is expected since the driving temperature difference for the air layer upward flow is higher for high permeability fabric case.

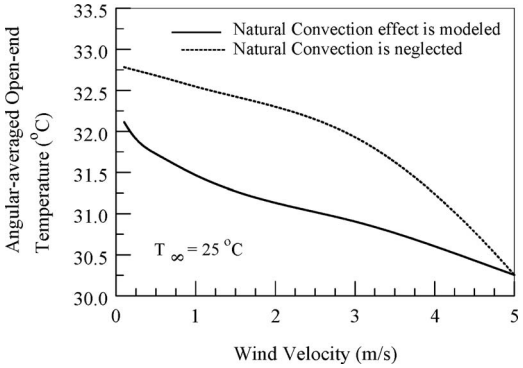

Fig. 8 A plot of the angular-averaged air temperature at the opening as a function of wind velocity at ambient condition of 25°C with and without natural convection effect for a fabric of permeability of 0.05 m/s

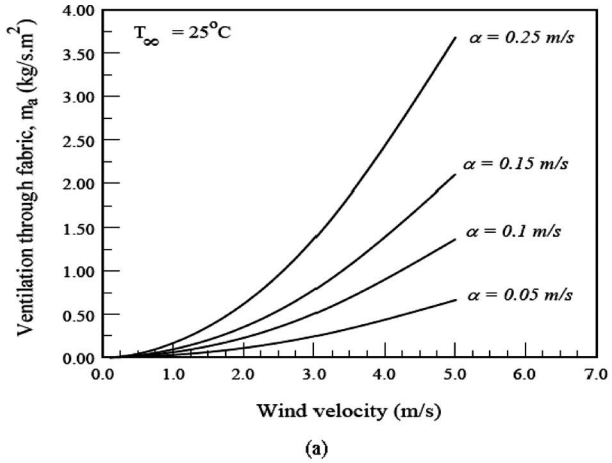

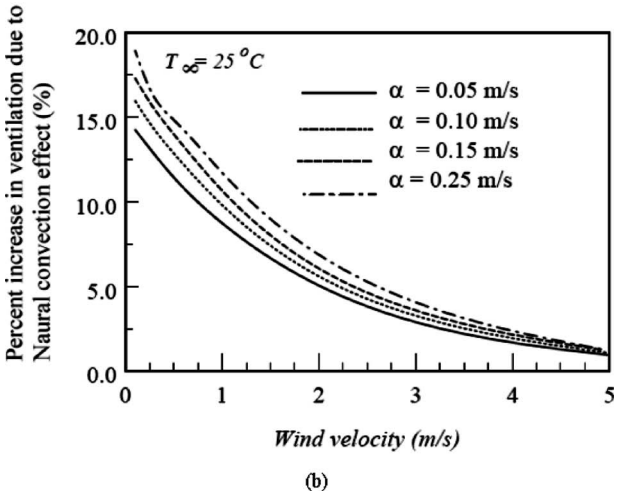

Fig. 9 Plot (*a*) the total ventilation rate through the fabric as predicted by the mixed convection model as a function of wind velocity at various fabric permeabilities and (*b*) the corresponding % increase in ventilation when natural convection is incorporated

The developed clothed cylinder ventilation and thermal model predicts the air ventilation, annulus air temperature, and sensible heat loss from the clothed cylinder that represents a clothed human trunk. The model can be extended to include latent heat loss, and if appropriately integrated with a segmented human bioheat model, it becomes an effective tool to predict the temperature variation and sweat distribution or nonuniformity of sweat rates over the trunk and the resultant effect on local thermal comfort.

5 Conclusions

This work presented from first principles the modeling of coupled ventilation and heat convection in a vertical air annulus between concentric fabric cylinder and heated solid cylinder placed in perpendicular to airflow. The effect of natural convection in annulus of clothed cylinder subject to external wind is important at low wind velocities where ventilation rates through the fabric and heat transfer show an increase of 15% and 12%, respectively, at wind velocities less than 1 m/s when natural convection was included in the modeling, depending on permeability.

Acknowledgment

The financial support of the Swedish Research Council—SIDA, the Lebanese National Council for Scientific Research, and of the

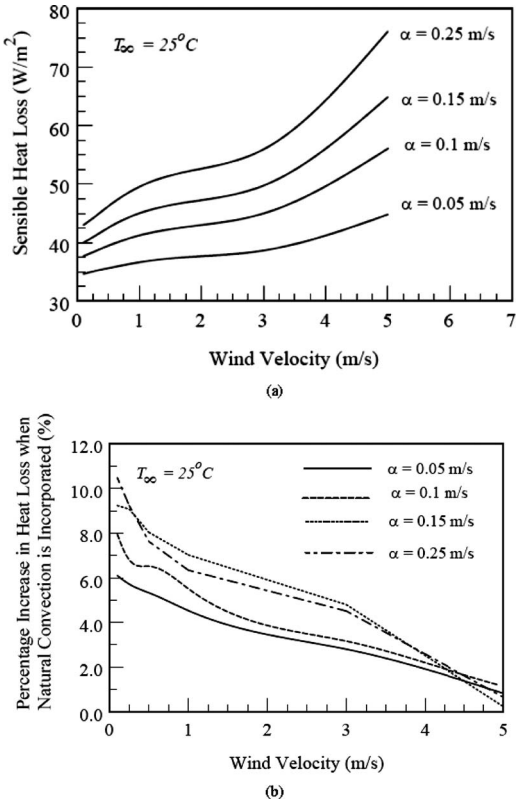

Fig. 10 Plots of the total heat loss through the fabric as predicted by the mixed convection model as a function of wind velocity at various fabric permeabilities

Qatar Chair in Energy Studies Endowment Fund are highly acknowledged.

Nomenclature

C_p = specific heat of air at constant pressure (J/kg K)
e_f = fabric cylinder thickness (m)
g = gravitational acceleration (m/s^2)
H'_{co} = effective convection heat transfer coefficient between outer node and air flowing through fabric (W/m^2 K)
h_c = heat transport coefficient from the fabric to the environment (W/m^2 K)
$h_{c(o-air)}$ = heat transport coefficient from the fabric to the trapped air layer (W/m^2 K)
$h_{c(skin-air)}$ = heat transport coefficient from the skin to the trapped air layer (W/m^2 K)
h_r = linearized radiative heat transfer coefficient (W/m^2 K)
k_a = thermal conductivity of air (W/m K)
L = fabric length in x direction (m)
$\dot{m}_{aY}$ = mass flow rate of air in radial direction (kg/m^2 s)
$\dot{m}_{ax}$ = mass flow rate of air in z-direction (kg/m^2 s)
$\dot{m}_{a\theta}$ = mass flow rate of air in θ-direction (kg/m^2 s)
$\dot{m}_o$ = net flow rate through the open aperture (kg/s)
$\dot{m}_{vent}$ = total ventilation rate in kg/s per m^2 of clothed body surface
P_a = air vapor pressure (kPa)
P_s = pressure at the external surface of the fabric (kPa)
P_∞ = atmospheric pressure (kPa)
Q_s = heat loss (W/m^2)
R_f = fabric cylinder radius (m)
R_s = inner cylinder radius (m)
T = temperature (°C)
V_∞ = velocity of the environment crosswind (m/s)
Y = air layer thickness (m)

Greek Symbols

α = fabric air permeability (m^3/m^2 s)
β = the volumetric thermal expansion coefficient ($°C^{-1}$)
ν = kinematic viscosity of air (m^2/s)
θ = angular coordinate

Subscripts

a = conditions of air in the annulus
o = fabric outer node
skin = conditions at the skin surface
void = local air inside the void
∞ = environment condition

References

[1] Mohanty, A. K., and Dubey, M. R., 1996, "Buoyancy Induced Flow and Heat Transfer through a Vertical Annulus," Int. J. Heat Mass Transfer, **39**(10), pp. 2087–2093.
[2] Oosthuizen, P. H., and Paul, J. T., 1986, "A Numerical Study of Free Convective Flow Through a Vertical Annular Duct," ASME Paper No. 86-WA/HT-81.
[3] A1-Arabi, M., E1-Shaarawi, E. A. I., and Khamis, M., 1987, "Natural Convection in Uniformly Heated Vertical Annuli," Int. J. Heat Mass Transfer, **30**, pp. 1381–1389.
[4] Sparrow, E. M., Chrysler, G. M., and Azevedo, A. F., 1984, "Observed Flow Reversals and Measured Predicted Nusselt Numbers for Natural Convection in a One-Sided Heated Vertical Channel," ASME J. Heat Transfer, **106**, pp. 325–332.
[5] Gebhart, B., Jaluria, Y., Mahajan, R. L., and Sammakia, B., 1988, *Buoyancy-Induced Flows and Transport*, Hemisphere, New York.
[6] Sobera, M. P., Kleijn, C. R., Brasser, P., and Van den Akker, H. E. A., 2003, "Convective Heat and Mass Transfer to a Cylinder Sheathed by a Porous Layer," AIChE J., **49**, pp. 3018–3028.
[7] Kind, R. J., Jenkins, J. M., and Seddigh, F., 1991, "Experimental Investigation of Heat Transfer Through Wind-Permeable Clothing," Cold Regions Sci. Technol., **20**, pp. 39–49.
[8] Gibson, P., Hill, R., Sobera, M. P., and Kleijn, C. R., 2006, "Computational Modeling of Clothing Performance," *Thermal and Moisture Transport in Fibrous Materials*, N. Pan and P. Gibson, eds., CRC, Boca Raton, FL, Chap. 15, pp. 546–553.
[9] Leong, J. C., and Lai, F. C., 2006, "Natural Convection in a Concentric Annulus With a Porous Sleeve," Int. J. Heat Mass Transfer, **49**, pp. 3016–3027.
[10] Chaves, C. A., Camargo, J. R., and Correa, V. A., 2008, "Combined Forced and Free Convection Heat Transfer in a Semi-Porous Open Cavity," Scientific Research and Essay, **3**(8), pp. 332–337, http://www.academicjournals.org/SRE.
[11] Ghaddar, N., Ghali, K., and Jreije, B., 2008, "Ventilation of Wind-Permeable Clothed Cylinder Subject to Periodic Swinging Motion," ASME J. Heat Transfer, **130**(9), p. 091702.
[12] Watanabe, T., Kato, T., and Kamata, Y., 1991, "The Velocity Distribution in the Inner Flow Field Around a Clothed Cylinder," Sen'i Gakkaishi, **44**(T-78), pp. 271–275.
[13] Bejan, A., 1995, *Convection Heat Transfer*, Wiley, New York.
[14] Ghali, K., Ghaddar, N., and Jaroudi, E., 2006, "Heat and Moisture Transport Through the Microclimate Air Annulus of the Clothing-Skin System Under Periodic Motion," ASME J. Heat Transfer, **128**(9), pp. 908–918.
[15] Reddy, V., and Narasimham, G., 2008, "Natural Convection in a Vertical Annulus Driven by a Central Heat Generating Rod," Int. J. Heat Mass Transfer, **51**, pp. 5024–5032.
[16] Ghali, K., Ghaddar, N., and Jones, B., 2002, "Multi-Layer Three-Node Model of Convective Transport Within Cotton Fibrous Medium," J. Porous Media, **5**(1), pp. 17–31.
[17] Ghali, K., Ghaddar, N., and Jones, B., 2002, "Empirical Evaluation of Convective Heat and Moisture Transport Coefficients in Porous Cotton Medium," ASME J. Heat Transfer, **124**(3), pp. 530–537.
[18] Holman, J. P., 1997, *Heat Transfer*, 8th ed., McGraw-Hill, NewYork, Chap. 8, pp. 488–491.
[19] Havenith, G., Heus, R., and Lotens, W. A., 1990, "Clothing Ventilation, Vapor Resistance and Permeability Index: Changes Due to Posture, Movement, and Wind," Ergonomics, **33**(8), pp. 989–1005.
[20] Lotens, W., 1993, "Heat Transfer From Humans Wearing Clothing," Ph.D. thesis, TNO Institute for Perception, Soesterberg, The Netherlands.